IMPROVED MODELING AND BOUNDS FOR NQR SPECTROSCOPY SIGNALS

G. Kyriakidou[1], A. Jakobsson[2], E. Gudmundson[2,3], A. Gregorovič[4], J. Barras[1], and K. Althoefer[1]

[1]Dept. of Informatics, King's College London, London, United Kingdom
[2]Dept. of Mathematical Statistics, Lund University, Lund, Sweden
[3]Swedish Defence Research Agency (FOI), Stockholm, Sweden
[4]Institute Jožef Stefan, Ljubljana, Slovenia

ABSTRACT

Nuclear Quadrupole Resonance (NQR) is a method of detection and unique characterization of compounds containing quadrupolar nuclei, commonly found in many forms of explosives, narcotics, and medicines. Typically, multi-pulse sequences are used to acquire the NQR signal, allowing the resulting signal to be well modeled as a sum of exponentially damped sinusoidal echoes. In this paper, we improve upon the earlier used NQR signal model, introducing an observed amplitude modulation of the spectral lines as a function of the sample temperature. This dependency noticeably affects the achievable identification performance in the typical case when the substance temperature is not perfectly known. We further extend the recently presented Cramér-Rao lower bound to the more detailed model, allowing one to determine suitable experimental conditions to optimize the detection and identifiability of the resulting signal. The theoretical results are carefully motivated using extensive NQR measurements.

Index Terms— Nuclear Quadrupole Resonance, temperature dependence, off-resonance effects, Cramér-Rao lower bound.

1. INTRODUCTION

Nuclear quadrupole resonance (NQR) is a radio-frequency (RF) spectroscopic method that detects and characterizes polycrystalline solid materials, containing quadrupolar nuclei, such as ^{14}N and ^{35}Cl, allowing for the detection and identification of a large range of chemical compounds [1–4]. The NQR signal is generated from the interaction of the sample property, the electric quadrupole moment, with the electric field gradient of the surrounding charges, such that proper application of RF pulses will drive transitions between the energy levels at particular frequencies, which are characteristic for each material [3, 5]. These measurements are commonly acquired using pulsed spin-locking (PSL) sequences for enhanced detection sensitivity. The PSL sequence consists of

a series of refocusing pulses phase shifted by $90°$ relative to the first preparatory pulse $\theta_{0°}^p$ [2, 6]. The RF pulses applied at equal time intervals, 2τ, refocus the transverse NQR magnetization, forming a train of M echoes as illustrated in Figure 1. The maximum signal intensity is acquired once the excitation frequency, ω_{exc}, of the RF pulses matches the spectral line of the quadrupolar nuclei, a condition known as *on-resonance* NQR detection. However, a notable reduction of the signal intensity may result if the signal is measured *off-resonance* [7], i.e., when

$$\Delta\omega_k = \omega_k - \omega_{exc} \neq 0 \qquad (1)$$

with the resonance frequency ω_k will typically be strongly temperature dependent. As shown in [7–9], the frequency dependencies of the NQR spectral lines follow a periodic (sinc-like) function with periodicity due to the RF pulse spacing τ. In NQR detection, and in particular, remote detection, the temperature of the material under study is only approximately known, and may also exhibit a noticeable temperature gradient across the substance, ensuring that the spectral lines and their intensities may be expected to vary substantially from their on-resonance values. The intensity of the spectral lines will also depend on the experimental parameters, such as the pulse spacing, pulse duration, sample quantity, and the type of pulse sequence used [7, 8, 10]. In this work, we exploit the model in [7] to improve the commonly used echo train NQR model proposed in [11] to incorporate the temperature dependency of the resonance frequency on the NQR signal, verifying the resulting model using measured NQR signals. Furthermore, we extend the Cramér-Rao lower bound (CRB) presented in [12] to the new data model, as well as illustrate the usability of the resulting expression for determining suitable experimental conditions to optimize detection and identification performance for a given setup and assumed temperature uncertainty. The rest of the paper is organized as follows: in the next section, we present the extended NQR model, followed in Section 3 by the derivation of the corresponding CRB. Then, in Section 4, we examine the usability of the presented bound to determine suitable experimental conditions. Finally, Section 5 contains our conclusions.
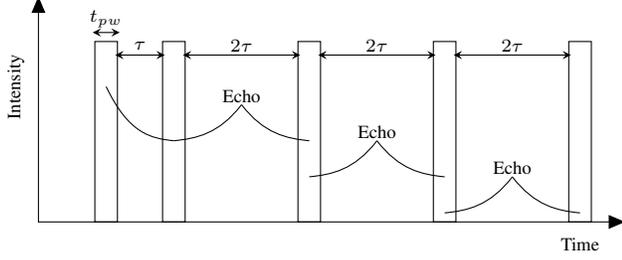
Fig. 1. The NQR signal formed using a PSL sequence.

2. THE NQR SIGNAL DATA MODEL

In this section, we extend the NQR model presented in [11], modeling the mth echo of an NQR signal resulting from a PSL excitation sequence as

$$y_{m,t} = x_{m,t} + v_{m,t} \quad (2)$$

where $v_{m,t}$ denotes an additive circularly symmetric Gaussian noise, typically being well modeled using a low-order autoregressive model [13], and with

$$x_{m,t} = \rho \sum_{k=1}^{K} s_k(\psi) e^{i\phi_k} e^{i\omega_k(T)t - \beta_k|t-\tau| - (t+2\tau m)\eta_k} \quad (3)$$

for echo number $m = 0, ..., M - 1$ and echo sampling times $t = t_0, ..., t_{N-1}$, with τ and K denoting the pulse interval and the number of NQR spectral lines, respectively. Here, the common scaling factor due to the signal-to-noise (SNR) ratio is given by ρ, whereas the (normalized) signal amplitude is described by $s_k(\psi)$, detailing the relative amplitudes of the K spectral lines. Furthermore, ϕ_k, β_k, and η_k denote the argument of the signal amplitude, the within echo decay and the echo train decay for the kth spectral line, respectively. In earlier works, $s_k(\psi)$ has been assumed to be a *constant* vector, which would not vary between experiments [11].

Here, we will modify this model such that $s_k(\psi)$ will be allowed to depend both on the used experimental setup and on the temperature of the examined substance, which will determine whether the measurement is on- or off-resonance, i.e.,

$$\psi = \begin{bmatrix} T & \tau & t_{pw} & \omega_{exc} & \omega_{nf} & \cos\theta \end{bmatrix}^{\mathrm{T}} \quad (4)$$

where $(\cdot)^T$ denotes the transpose, and with T, t_{pw}, ω_{exc}, ω_{nf}, and θ denoting the temperature of the substance, the pulse length, the excitation frequency, the nutation frequency of the RF field created by the coil, along its axis, and the angle that the RF pulse field makes with the coil's axis, respectively. Using the model for the temperature dependency of $s_k(\psi)$ presented in [7], where the steady state signal amplitude dependence on the off-resonance effects was proposed and validated using extensive experimental observations of paranitrotoluene (PNT), the signal amplitude may be modeled as (see

also [8, 14–16])

$$s_k(\psi) = \zeta M \int_0^1 \cos\theta \, n_1 \, n_2^2 \, d(\cos\theta) \quad (5)$$

where ζ is a constant, and assuming that $2\tau \leq T_{2e}$, with T_{2e} denoting the effective relaxation time constant of the decaying echo train, and

$$n_1 = \frac{2\omega_{1\theta} \sin(\tilde{\omega}_{1\theta} t_{pw})}{\tilde{\omega}_{1\theta}} \quad (6)$$

$$n_2 = \frac{\omega_{1\theta} \sin\left(\frac{1}{2}\tilde{\omega}_{1\theta} t_{pw}\right)}{\tilde{\omega}_{1\theta} \sqrt{1 - \cos^2\left(\frac{1}{2}\Omega t_c\right)}} \quad (7)$$

with

$$\cos\left(\frac{1}{2}\Omega t_c\right) = \cos(\Delta\omega_k \tau) \cos\left(\frac{1}{2}\tilde{\omega}_{1\theta} t_{pw}\right)$$
$$- \frac{\Delta\omega_k}{\tilde{\omega}_{1\theta}} \sin(\Delta\omega_k \tau) \sin\left(\frac{1}{2}\tilde{\omega}_{1\theta} t_{pw}\right)$$

with the constants $\omega_{1\theta} = \omega_{nf} \cos\theta$, $t_c = 2\tau + t_{pw}$, and

$$\tilde{\omega}_{1\theta} = \sqrt{\Delta\omega_k^2 + \omega_{1\theta}^2} \quad (8)$$

It should be noted that as the decay of the signal echoes will depend strongly on the used pulse repetition interval, τ, and pulse length, t_{pw}, the number of usable echoes, to obtain optimum SNR, will be about (see also [7, 10, 14])

$$M = 1.25 \frac{T_{2e}}{t_c} = 1.25 \frac{T_{2e}}{2\tau + t_{pw}} \quad (9)$$

The temperature dependent NQR resonance frequencies may be well modeled as [13, 17, 18]

$$\omega_k(T) = a_k - b_k T \quad (10)$$

with a_k and b_k being the known constants depending on the examined substance. It may be noted that (6) indicates the offset effects occurring during the first preparatory pulse, whereas (7) yields the offset for the remainder of the RF pulses. Figure 2 illustrates a typical amplitude function for varying frequency offset, here for the substance sodium nitrate, for the spectral line of 3.6 MHz ($K = 1$), as obtained using (5). Clearly, the offset variations, with periodicity t_c^{-1}, substantially affect the expected signal magnitude, also revealing, as expected, the maximum intensity at $\Delta\omega = 0$. It must be noted from the figure that the SNR will be substantially reduced even for an off-resonance frequency of 500 Hz. In addition, the NQR signal intensity modulation exhibits minimum and maximum values at $\Delta\omega_k = 2\pi(n + 1/2)/t_c$ and $\Delta\omega_k = 2\pi n/t_c$, respectively, with $n = 0, \pm1, \pm2, ...$ (see also [7, 10]). Finally, the presented NQR model will be overall controlled by the effect of the bandwidth of the quality-factor (Q) of the coil. In this work, we have, for simplicity, assumed that the Q-factor has been selected sufficiently large to make this effect negligible.
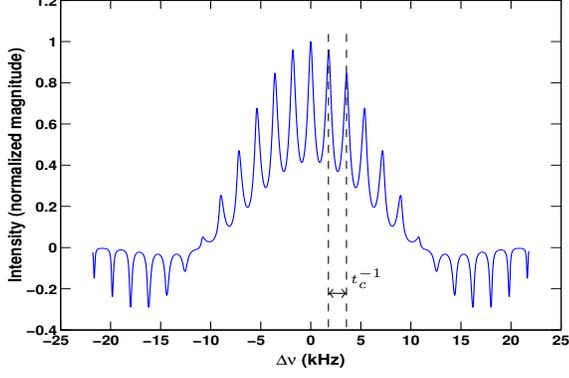
Fig. 2. Theoretical model of the NQR signal magnitude as a function of the frequency offset, $\Delta\omega = 2\pi\Delta\nu$, for a PSL sequence, using the 3.6 MHz spectral line of sodium nitrate as the sample model.

3. THE CRAMÉR-RAO LOWER BOUND

We proceed to derive the CRB for the extended model in (3), using (5). For simplicity, the mth signal echo may be rewritten as

$$x_{m,t} = \sum_{k=1}^{K} \rho\, s_k(\boldsymbol{\psi})\, e^{i\phi_k}\, \lambda_k^{m,t} \tag{11}$$

with

$$\lambda_k^{m,t} \triangleq e^{iw_k t - \beta_k|t-\tau| - (t+2\tau m)\eta_k} \tag{12}$$

Gathering the available NM measurements on a vector form, the NQR echo train may be expressed as

$$\mathbf{y}_{NM} = \mathbf{x}_{NM} + \boldsymbol{\upsilon}_{NM} \tag{13}$$

where

$$\mathbf{x}_{NM} = \begin{bmatrix} \mathbf{x}_0^{\mathrm{T}} & \dots & \mathbf{x}_{M-1}^{\mathrm{T}} \end{bmatrix}^{\mathrm{T}} \tag{14}$$

$$\mathbf{x}_m = \begin{bmatrix} x_{m,t_0} & \dots & x_{m,t_{N-1}} \end{bmatrix}^{\mathrm{T}} \tag{15}$$

$$\boldsymbol{\upsilon}_{NM} = \begin{bmatrix} \upsilon_{0,t_0} & \dots & \upsilon_{M-1,t_{N-1}} \end{bmatrix}^{\mathrm{T}} \tag{16}$$

Using the Slepian-Bang's formula [19], the CRB may be computed as

$$\mathbf{CRB} = \frac{\sigma^2}{2}\left[Re\left\{ \left(\frac{\partial \mathbf{x}}{\partial \boldsymbol{\gamma}}\right)^H \left(\frac{\partial \mathbf{x}}{\partial \boldsymbol{\gamma}}\right) \right\} \right]^{-1} \tag{17}$$

where $(\cdot)^H$ denotes the Hermitian conjugate transpose, σ^2 the variance of $\mathbf{v}_{NM}$, and $\boldsymbol{\gamma}$ the unknown parameters, i.e.,

$$\boldsymbol{\gamma} = \begin{bmatrix} \rho & T & \boldsymbol{\phi}^{\mathrm{T}} & \boldsymbol{\beta}^{\mathrm{T}} & \boldsymbol{\eta}^{\mathrm{T}} \end{bmatrix}^{\mathrm{T}} \tag{18}$$

$$\boldsymbol{\phi} = \begin{bmatrix} \phi_1 & \dots & \phi_K \end{bmatrix}^{\mathrm{T}} \tag{19}$$

$$\boldsymbol{\beta} = \begin{bmatrix} \beta_1 & \dots & \beta_K \end{bmatrix}^{\mathrm{T}} \tag{20}$$

$$\boldsymbol{\eta} = \begin{bmatrix} \eta_1 & \dots & \eta_K \end{bmatrix}^{\mathrm{T}} \tag{21}$$
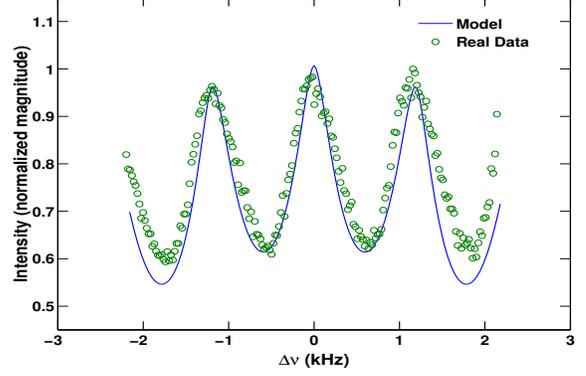

Fig. 3. Comparison of experimental and theoretical signal intensities as a function of the frequency offset.

and with the derivatives with respect to the elements in $\boldsymbol{\gamma}$ given by

$$\frac{\partial x_{m,t}}{\partial \rho} = \sum_{k=1}^{K} s_k(T)\, e^{i\phi_k} \lambda_k^{m,t}$$

$$\frac{\partial x_{m,t}}{\partial T} = \rho \sum_{k=1}^{K} \left(\frac{\partial s_k(T)}{\partial T} - i\, t\, b_k\, s_k(T) \right) e^{i\phi_k} \lambda_k^{m,t}(T)$$

$$\frac{\partial x_{m,t}}{\partial \phi_k} = i\, \rho\, s_k(T)\, e^{i\phi_k} \lambda_k^{m,t}$$

$$\frac{\partial x_{m,t}}{\partial \beta_k} = -\rho\, |t-\tau| s_k(T)\, e^{i\phi_k} \lambda_k^{m,t}$$

$$\frac{\partial x_{m,t}}{\partial \eta_k} = -\rho\, (t+2\,\tau\, m)\, s_k(T)\, e^{i\phi_k} \lambda_k^{m,t}$$

In the following numerical study, we have, given the convoluted expression of $s_k(T)$, evaluated the partial derivative $\partial s_k(T)/\partial T$ numerically.

4. NUMERICAL RESULTS

In order to validate the NQR echo train model in (3), we performed experimental measurements of the signal intensities for the 3.6152 MHz spectral line of sodium nitrate at varying frequency offsets. The powder sample of sodium nitrate was immersed in a silicone oil to reduce the piezoelectric effects. This is illustrated in Figure 3, with the data being measured using $M = 128$ echoes, $N = 64$ data acquisition points per echo, $\tau = 407\,\mu\text{sec}$, $t_{pw} = 40\,\mu\text{sec}$, and $\omega_{nf} = 52\,\text{kHz}$. The temperature shifting constants for this spectral line are $a_1 = 3.924\,\text{MHz}$, and $b_1 = 1.09\,\text{kHz/K}$. As shown in the figure, the results reveal a reasonably good agreement between the model and the experimental data yielding an accurate prediction of the expected amplitude as the frequency offset varies. It should be stressed that the theoretical model is calculated from the experimental parameters of the PSL sequence, and the quadrupolar characteristics of the substance,

with no fitting performed on the real data. Proceeding, we illustrate the usability of the derived CRB in determining a proper measurement setup. In practice, NQR may be used to quantify the active pharmaceutical ingredient present in a substance, allowing, for instance, for the detection of substandard or counterfeit medicines, which normally do not contain the expected quantity [2]. Thus, it is important to estimate the expected signal amplitude under several effects, for accurate quantitative results. For our case, with a signal where the additive noise may be well approximated as being a white Gaussian noise, the estimated amplitudes may be expected to lie within three standard deviations of the true amplitude with 99% probability. However, as the standard deviation is generally unknown, we here form an estimate of the corresponding confidence interval by using the CRB of the signal magnitude, ρ, as a measure of the variance of the signal amplitude. Such a case is illustrated in Figure 4, which shows the required number of echo trains (accumulations) one may need to achieve a sufficiently strong SNR, with respect to the corresponding desired estimation accuracy. The NQR parameters, β_k, η_k, ρ and the noise variance were estimated using the echo train maximum likelihood (ETAML) detection algorithm proposed in [11], by taking the average over 32 accumulations. These parameters were then used as the true parameters for the computation of the CRB. In Figure 4, the real data were acquired and accumulated 32 times, for the on-resonance case ($\Delta\omega = 0$) at $T = 283$ K, using the experimental parameters for the same sample, sodium nitrate, as described above. The measurements were then averaged using a cross-validation scheme, as shown in Figure 4. Starting from the bottom line, the real data points of the amplitude estimation error were computed from each of the 32 measurements. The second line shows 32 data points, each of which is the average of two measurements, chosen at random among the 32 accumulations. Similarly, the third line is the result of averaging three measurements, etc., up to 31 averaged data points. The mean amplitude estimate was then used as the true amplitude for the CRB computation. As expected, the CRB is seen to accurately yield the expected variability for the on-resonance case, i.e., when no temperature uncertainty is assumed ($\Delta T = 0$ K). In order to test how the estimation accuracy is affected by the presence of uncertainty in the assumed temperature of the substance, the CRB was computed for the cases of $\Delta T = 0.5$ K and $\Delta T = 1.5$ K, which correspond to the first two minima of the amplitude modulation model in Figure 3. As shown in Figure 4, the CRB variability increases dramatically even for the small deviation of $\Delta T = 0.5$ K from the assumed temperature. In particular, the expected signal magnitude drops off approximately two times as compared to the maximum NQR signal amplitude for the on-resonance case. Thus, in the presence of off-resonance effects, one may need to acquire more echo trains to achieve a sufficient estimation accuracy to the same level, prolonging the experimental durations.
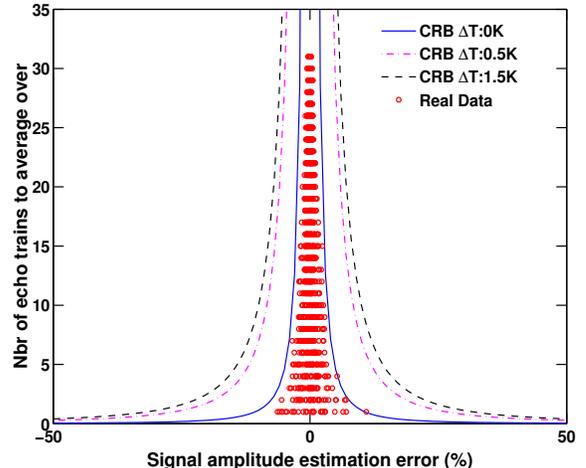

Fig. 4. The 99% estimation accuracy as determined using the CRB of the NQR signal intensity at different offset frequencies. The theoretical bounds are compared with NQR measurements on sodium nitrate, for the 3.6 MHz spectral line.

5. CONCLUSION

In this paper, we have extended the current state-of-the-art NQR echo train data model to incorporate the temperature dependence of the resonance frequencies and signal amplitudes. This recently determined dependency will strongly affect the expected intensity of the NQR signal, profoundly affecting the performance of existing detection and identification algorithms. The refined model allows such algorithms to take this effect into account, as an accurate modeling of the expected signal intensities, and the corresponding estimation variance, given an expected uncertainty in the assumed temperature of the substance. Such an uncertainty can often be as much as 0.5 K, which would affect the resulting SNR. The presented model was compared and validated using the measured signal intensities of the substance, sodium nitrate. Furthermore, the CRB of the refined model was derived and compared to the variability observed in the sodium nitrate data. As illustrated in the paper, the presented results may, for instance, be used to determine the number of signal averages required to achieve a desired estimation accuracy, given an expected uncertainty in the assumed temperature of the substance.

6. ACKNOWLEDGEMENT

REFERENCES

[1] J. Barras, K. Althoefer, M. D. Rowe, I. J. Poplett, and J. A. S. Smith, "The Emerging Field of Medicines Authentication by Nuclear Quadrupole Resonance Spectroscopy," *Appl. Magn. Reson.*, vol. 43, pp. 511–529, 2012.

[2] E. Balchin, D. J. Malcolme-Lawes, I. J. F. Poplett, M. D. Rowe, J. A. S. Smith, G. E. S. Pearce, and S. A. C. Wren, "Potential of Nuclear Quadrupole Resonance in Pharmaceutical Analysis," *Anal. Chem.*, vol. 77, pp. 3925–3930, 2005.

[3] J. N. Latosinska, "Applications of nuclear quadrupole resonance spectroscopy in drug development," *Expert Opinion on Drug Discovery*, vol. 2, no. 2, pp. 225–248, 2007.

[4] N. R. Butt, E. Gudmundson, and A. Jakobsson, "An Overview of NQR Signal Detection Algorithms," in *Magnetic Resonance Detection of Explosives and Illicit Materials*, T. Apih, B. Rameev, G. Mozzhukhin, and J. Barras, Eds., NATO Science for Peace and Security Series B: Physics and Biophysics, pp. 19–33. Springer Netherlands, 2014.

[5] S. C. Pérez, L. Cerioni, A. E. Wolfenson, S. Faudone, and S. L. Cuffini, "Utilisation of Pure Nuclear Quadrupole Resonance Spectroscopy for the Study of Pharmaceutical Forms," *Int. J. Pharm.*, vol. 298, pp. 143–152, 2005.

[6] M. W. Malone, M. McGillvray, and K. L. Sauer, "Revealing dipolar coupling with NQR off-resonant pulsed spin locking," *Phys. Rev. B*, vol. 84, pp. 214430, 2011.

[7] A. Gregorovič and T. Apih, "Relaxation during spin-lock spin-echo pulse sequence in 14N nuclear quadrupole resonance," *J. Chem. Physics*, vol. 129, pp. 214504, 2008.

[8] A. Gregorovič and T. Apih, "Improving 14N nuclear quadrupole resonance detection of trinitrotoluene using off-resonance effects," *Solid State Nucl. Magn. Reson.*, vol. 36, pp. 96–98, 2009.

[9] T. N. Rudakov, V. T. Mikhaltsevitch, P. A. Hayes, and W. P. Chisholm, "Some Dynamical Properties of Nitrogen-14 Quadrupolar Spin-System with Non-Symmetric Electric Field Gradient Tensor," *Chem. Phys. Lett.*, vol. 387, pp. 405–409, 2004.

[10] A. Gregorovič, T. Apih, J. Lužnik, J. Pirnat, and Z. Trontelj, ^{14}N *Nuclear Quadrupole Resonance Signals in Paranitrotoluene and Trinitrotoluene. Spin-Lock Spin-Echo Off-Resonance Effects*, Springer, 2009.

[11] S. D. Somasundaram, A. Jakobsson, J. A. S. Smith, and K. Althoefer, "Exploiting Spin Echo Decay in the Detection of Nuclear Quadrupole Resonance Signals," *IEEE Trans. Geosci. Remote Sens.*, vol. 45, no. 4, pp. 925–933, April 2007.

[12] E. Gudmundson, P. Wirfält, A. Jakobsson, and M. Jansson, "An ESPRIT-based parameter estimator for spectroscopic data," in *Proc. IEEE Stat. Signal Process. Workshop (SSP'12)*, Ann Arbor, Michigan, USA, Aug. 5-8 2012.

[13] A. Jakobsson, M. Mossberg, M. Rowe, and J. A. S. Smith, "Exploiting Temperature Dependency in the Detection of NQR Signals," *IEEE Trans. Signal Process.*, vol. 54, no. 5, pp. 1610–1616, May 2006.

[14] R. A. Marino and S. M. Klainer, "Multiple spin echoes in pure quadrupole resonance," *J. Chem. Phys.*, vol. 67, no. 7, pp. 3388, October 1977.

[15] V. T. Mikhaltsevitch and T. N. Rudakov, "On the NQR Detection of Nitrogenated Substances by Multi-Pulse Sequences," *Physica Status Solidi (b)*, vol. 241, pp. 411–419, 2004.

[16] R. S. Cantor and J. S. Waugh, "Pulsed Spin-locking in Pure Nuclear Quadrupole Resonance," *J. Chem. Phys.*, vol. 73, no. 2, pp. 1054–1063, August 1980.

[17] J. A. S. Smith, M. D. Rowe, R. M. Deas, and M. J. Gaskell, "Nuclear Quadrupole Resonance Detection of Landmines," in *Proc. Int. Conf. Requir. Technol. Detect., Remov. Neutralization Landmines UXO*, H. Sahli, A. M. Bottoms, and J. Cornelis, Eds., Brussels, Belgium, September 15-18 2003, vol. 2, pp. 715–721.

[18] R. M. Deas, M. J. Gaskell, K. Long, N. F. Peirson, M. D. Rowe, and J. A. S. Smith, "An NQR study of the crystalline structure of TNT," in *SPIE Def. Secur. Symp.*, 2004.

[19] P. Stoica and R. Moses, *Spectral Analysis of Signals*, Prentice Hall, Upper Saddle River, N.J., 2005.